Preprint, 2019

Further Insights on the Relationship Between SP500, VIX and Volume: A New Asymmetric Causality Test[1]

by

Catherine Kyrtsou(1), Dimitris Kugiumtzis(2) and Angeliki Papana(2)

[1]University of Macedonia, CAC IXXI-ENS Lyon, University of Paris 10 (EconomiX), (ckyrtsou@uom.gr), *corresponding author*
[2]Faculty of Engineering, Aristotle University of Thessaloniki, Greece (dkugiu@auth.gr), (angeliki.papana@gmail.com)

Abstract

In the aim to explore the complex relationships between S&P500, VIX and volume we introduce a Granger causality test using the nonlinear statistic of Asymmetric Partial Transfer Entropy (APTE). Through a simulation exercise, it arises that the APTE offers precise information on the nature of the connectivity. Our empirical findings concretize the information flow that links volume, S&P500 and VIX, and merge the leverage effect and the asymmetric stock return-volume relationship into a unified framework of analysis. More specifically, when we condition on the tails, the detected causal channel provides empirical validation of the noise trading contribution to large swings in financial markets, because of the increase of trading volume and the subsequent worsening ability of market prices to adjust to new information.

Keywords: Asymmetry, direct Granger causality, leverage effect, stock return-volume relationship.

JEL codes: C32, C58, G10

[1] The authors would like to thank the participants of the 12th Biennial Athenian Policy Forum Conference, on Economic and Financial Asymmetries, National Debts and Government Policies, in Toronto, June 13-14, 2014, for their helpful comments.
The research project is implemented within the framework of the Action Supporting Postdoctoral Researchers of the Operational Program Education and Lifelong Learning (Actions Beneficiary: General Secretariat for Research and Technology), and is co-financed by the European Social Fund (ESF) and the Greek State.

1. Introduction

There is significant evidence that the evolution of the role of speculation and investors' expectations built up a strong nonlinear connectivity among financial variables. Supported by bubbly liquidity and leverage, modern financial markets were evolved as networks of interacting entities. Likewise, the presence of phenomena such as information asymmetry, clustering and small world property provided additional indication of profound similarities between complex and financial networks.

The symmetry breaking in systems with variables being the nodes of a complex network, the resulting propagation mechanism and its contribution to the creation of long tail probability distribution reveal insightful dimensions of financial market's underlying dynamics. The asymmetric arrival of news and interpretation of shocks lie behind well-known relationships reported in the literature such as: i) the leverage effect (Black, 1976): negative shocks to stock returns drive up volatility, ii) the volatility feedback hypothesis (Poterba and Summers, 1986; Cambell and Hentschel, 1992): positive volatility changes lead to decreasing stock returns, iii) the positive stock return-volume relationship (DeLong et al., 1990), as well as iv) the asymmetric association of stock returns and volume of Cambell et al., (1993): a stock price decline on a high-volume day is more likely than a stock price decline on a low-volume day. Methodologically, alternative approaches have been suggested in the literature to analyse the interactions between index returns, volatility and volume. Recent examples include Chiang (2012), Dufour et al., (2012), He et al., (2014), He and Wen (2015), Slim and Dahmene (2016).

Indeed, theoretical and empirical evidence puts forward the nonlinearity and complexity of interdependence between financial variables. Among the battery of tools we have at our disposal to quantify interdependence, Granger causality presents significant advantages. It regards directed interdependence in a pair of variables (X,Y) by quantifying the predictive information X can contribute for the prediction of Y. While originally Granger causality was defined in terms of linear autoregressive models (Granger, 1969; Geweke, 1982), in the two last decades it was extended in different nonlinear settings. The most appealing form of Granger causality is based on information theory, and particularly the measure of transfer entropy (TE) (Schreiber, 2000) because it is model-free and of general purpose (quantifying both linear and nonlinear causal effects). The simplest approach for the detection of causal effects among a set of variables is to apply causality tests using a bivariate causality statistic like TE, where for all combinations of pairs of time series each pair (X,Y) is examined independently in terms of the existence, strength and direction of their coupling. However, in real financial systems, it is important that all the available information from the set of variables is taken into account. To do so, the concept of direct causality is introduced, meaning that the causal effect from X to Y is examined in view of the causal effects of other variables to Y. To address direct causality many bivariate causality measures have been modified, e.g. TE has been extended to partial TE (PTE) (Vakorin et al, 2009; Papana et al, 2012). As mentioned by Dufour et al., (2012) "the identification of a causal relationship depends crucially on the specification of the information set". The application of direct causality tests, e.g. significance test for PTE, prevents from spurious results that may be derived when constraining the analysis on couples and ignoring information from the remaining variables. This problem is addressed among others by Hsiao (1982), Pearl (2009) and Eichler (2016).

On the basis of connectivity between the S&P500 index, the CBOE Volatility Index (VIX) and the volume of S&P500, the goal of this paper is to map the dynamics of the US stock exchange. The rich informational content of the VIX, characterised as a fear gauge by Whaley (2000), and the trading volume, serving as a proxy for noise traders activity (Duffee, 1992) make them the best candidate variables for an in-depth behavioural analysis of the market swings. In terms of methodology, the selected direct causality measures of TE and PTE are modified so as asymmetry on top of nonlinearity can be appropriately captured and interpreted. In particular, we introduce an asymmetric version of the Transfer Entropy (ATE) and its partial variant (APTE). ATE (APTE) is considered as the test statistic for the null hypothesis of non-asymmetric causality. The inclusion of asymmetry prevents from otherwise spurious no rejection of causality, since the joint presence of positive and negative causal effects may cancel out each other (Chuang et al., 2009). Our empirical findings concretize the information flow that links volume, S&P500 and VIX, and merge the leverage effect and the asymmetric stock return-volume relationship into a unified framework of analysis.

The reminder of the paper is as follows. In Section 2 we review the causality measures forming the basis for the proposed asymmetric causality measures, we discuss the differences between indirect and direct causality, and then we present the asymmetric Transfer Entropy and partial Transfer Entropy tests (ATE/APTE). Section 3 and 4 include the simulation exercise and the respective results. Section 5 refers to the application of APTE to financial time series, while Section 6 concludes the paper.

2. Methodology

2.1. Brief Survey

A wide range of causality tests have been studied and developed attempting to identify causal relationships among real variables. Nevertheless, Granger causality has been so far the leading concept (Granger, 1969). Linear extensions include asymmetric causality (Hatemi-J, 2012; He et al., 2014), conditional or partial variants (Guo et al., 2008), partial directed coherence (Baccala and Sameshima, 2001) and direct directed transfer function (Blinowska et al, 2004).

Since financial and economic time series are complex and contain nonlinearities, we are interested in nonlinear causality, and specifically in information-theoretic methods that constitute a valid, model-free approach to assess nonlinear causality for both deterministic and stochastic systems. They incorporate the flow of time into the desired measure through the utilization of conditional (transition) probabilities. The nonlinear causality measures can be split into five main categories: i) those exploiting the direction of the flow of time to achieve a causal ordering of the dependent variables (e.g. Diks and Panchenko, 2006) ii) synchronization metrics based on the relative timings of events or the conformity of the rhythms of two oscillators (Quian Quiroga et al., 2000; Rosenblum and Pikovsky, 2001), iii) state space measures that use neighbourhood distances of reconstructed points (Arnhold et al., 1999; Romano et al., 2007), iv) information measures, defined in terms of entropies and probability distribution functions (Schreiber 2000; Vlachos and Kugiumtzis 2010), and v) model-based techniques testing for nonlinear and asymmetric feedbacks (Faes et al., 2008; Hristu-Varsakelis and Kyrtsou, 2008).

The new tool of partial transfer entropy (PTE) is the extension of the bivariate transfer entropy (TE) to multivariate time series (Schreiber 2000). Though TE has been used extensively in applications in the last decade, PTE was presented only very recently (Vakorin et al., 2009; Papana et al., 2012). Applications in finance and economics include Papana et al., (2013), Kyrtsou et al., (2013), Kyrtsou et al., (2016) and Papana et al., (2017).

The advantage of partial causality tests to detect direct causal relationships in multivariate systems can be visually represented in the following example. In Figure 1 we present a trivariate system composed of X, Y and Z, where X→Y and Y→Z. If a causality test is applied using a bivariate test statistic such as TE, it will identify the two true direct causal effects X→Y and Y→Z (solid lines) as well as the indirect causality from X to Z (dashed line). In contrast, if the test uses a multivariate causality measure, such as PTE, it will identify only the true causal couplings X→Y and Y→Z. In epidemiology, X is defined as "risk factor" (Merrill and Timmreck, 2006).

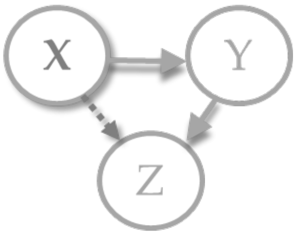

Figure 1: Path diagram for the visualisation of causal effects in a trivariate system.

2.2 *The Asymmetric Transfer Entropy (ATE) and its partial variant (APTE)*

The transfer entropy (TE) is a non-parametric measure that expresses the amount of information transferred from one observed variable X_2 to another observed variable X_1 (Schreiber, 2000). The two variables may represent coupled (or uncoupled) dynamical systems or stochastic processes. The TE from X_2 to X_1 is the amount of additional information about the future values of X_1 provided by knowing past values of X_1 and X_2 instead of past values of X_1 alone. We consider the delay vectors $\boldsymbol{x}_{1,t} = (x_{1,t}, x_{1,t-\tau}, \dots, x_{1,t-(m-1)\tau})'$ and $\boldsymbol{x}_{2,t} = (x_{2,t}, x_{2,t-\tau}, \dots, x_{2,t-(m-1)\tau})'$ of the bivariate time series $\{x_{1,t}, x_{2,t}\}, t = 1, \dots, n$, where m is the embedding dimension and τ is the time delay. The TE is a bivariate measure of causality, defined in terms of transition probabilities and therefore provides information about the direction of the dependencies. Specifically, the TE from X_2 to X_1 is the conditional mutual information $I(x_{1,t+1}; \boldsymbol{x}_{2,t} | \boldsymbol{x}_{1,t})$:

$$TE_{X_2 \to X_1} = \sum p(x_{1,t+1}, \boldsymbol{x}_{2,t}, \boldsymbol{x}_{1,t}) log \frac{p(x_{1,t+1} | \boldsymbol{x}_{1,t}, \boldsymbol{x}_{2,t})}{p(x_{1,t+1} | \boldsymbol{x}_{1,t})},$$

where TE is given based on the marginal and joint probability distributions, and the sum is over all possible states of ($x_{1,t+1}$,$\boldsymbol{x}_{2,t}$,$\boldsymbol{x}_{1,t}$) assuming a suitable partition.

The partial transfer entropy (PTE) is the extension of the TE in the multivariate case. The PTE accounts for the direct coupling of a variable X_2 to a variable X_1 conditioning on the confounding variables $Z=X_3, X_4,\dots,X_K$. It is defined similarly to TE:

$$PTE_{X_2\rightarrow X_1|Z} = I\left(x_{1,t+1};\boldsymbol{x}_{2,t}|\boldsymbol{x}_{1,t},\boldsymbol{z}_t\right)$$

where $\mathbf{z}_t$ comprises the delay vector of the K-2 conditioning variables in Z. For the computation of the aforementioned measures, it is suggested to utilize the nearest neighbour estimator that has been proved to be robust (Papana et al., 2012).

The TE identifies the causality relationship between the pair of variables X_1 and X_2, while the PTE captures the direct couplings. However, one might be interested in looking at whether these relationships hold when conditioning for a subset of the original observations. More specifically, we focus on whether positive observations of X_2 give predictive information about X_1 that is more significant than that provided by negative ones. In this effort, we expand the TE/PTE in order to allow detection of causal effects between two processes after considering the signs of the time series (assuming that the time series are given or converted to differences from a reference level). The asymmetric TE (ATE) and the asymmetric PTE (APTE) can be defined accordingly: an observation $\mathrm{x}_{2\mathrm{t}}$ of X_2 is included in the estimation of $ATE_{X_{2+}\rightarrow X_1}/APTE_{X_{2+}\rightarrow X_1|Z}$ only if $x_{2,t}\geq 0$ or equivalently only if $\mathrm{x}_{2,\mathrm{t}}<0$ (along with the corresponding observations x_{1t} of X_1). Alternatively, this conditioning can be further developed so that one can quantify the asymmetric causality based on the values from the tails of the distribution. In that case, the asymmetric causality measures are calculated using only the observations that satisfy appropriate conditions, e.g. values that lie further than one standard deviation above or below the mean.

2.3 Causality test based on ATE/APTE

Theoretically, a causality measure should be zero in case of no causal effects and otherwise be positive. Due to estimation bias, e.g. bias in the estimation of entropies in the conditional mutual information in TE and PTE, this never applies. Thus, a significance test for the causality measure is required in order to decide whether a causal relationship exists. Thus to examine the causal relationship from X_2 to X_1, the null hypothesis of the test is that there is no causality from X_2 to X_1 and the test statistic is the causality measure, e.g. $TE_{X2\rightarrow X1}$.

The statistical significance of ATE/APTE is assessed using a resampling method because the null distribution is not known (e.g. see Vicente et al., 2011; Papana et al., 2013; Papana et al., 2017). Specifically, we create M surrogate time series consistent with the non-causality null hypothesis H_0, i.e., that X_2 does not Granger causes X_1. To do so, we employ time-shifted surrogates (Quian Quiroga et al, 2002); a number *d* is randomly chosen from {1+e,2+e,…,n-1-e, n-e}, where n is the time series length and e a small time offset, and the *d*-first values of the time series X_2 are moved to the end, keeping the time series of X_2 unchanged. The corresponding causality measure is computed on the original time series, denoted as q_0, and on each of M surrogate time series, represented by $q_1, q_2, \dots, q_M$. If q_0 is at the tail of the empirical null distribution formed by $q_1, q_2, \dots, q_M$, then H_0 is rejected. The p-value from the one-sided test equals $1 - \frac{r_0 - 0.326}{M+1+0.348}$, where r_0 is the rank of q_0 when ranking in ascending order the list $q_0, q_1, q_2, \dots, q_M$ (the correction for the empirical cumulative function suggested in Yu and Huang (2001) is used). If the estimated p-value is ≤ 0.05, then a significant causal relationship exists. For the multivariate measures, the resampling test is formed in the same way, leaving the time series of the other variables in Z intact.

3. Simulation study

The performance of the ATE/APTE is evaluated through simulation experiments. Coupled systems with symmetric and asymmetric causality are considered including both linear and nonlinear couplings. For comparison reasons, we also estimate the original causality tests on TE/PTE. 100 realizations are generated from each system[2]. We set the time series lengths n=1000, 2000, 4000, embedding dimension m=1 (m=2 and τ=1 for system 1) and number of neighbors k=5. As reported in Kraskov et al., (2004) and Vlachos and Kugiumtzis (2010) the k-nearest neighbours method is not significantly affected by the choice of k.

The bivariate causality measures TE/ATE are tested on the simulation systems 1 – 4, while the multivariate measures PTE/APTE are applied to the simulation systems 5-8.

[2] The goal of the simulation exercise is to demonstrate whether the inclusion of asymmetry into a well-known measure, such as the transfer entropy, can provide further information when financial data are used. We do not draw conclusions based solely on the percentages of rejection of the null hypothesis of non-causal effects. In many statistical simulations, involving typically computations of low time cost, the number of realizations is often very high in order to arrive to safe estimations. For simulations involving nonlinear methods that are computationally intensive the number of realizations is much smaller and the use of 100 realizations in this case is rather the common practice and a good trade-off of statistical significance of the results and time efficiency. The computation of transfer entropy is indeed time intensive. Similar setting is common in simulation studies presented by Faes et al., (2011), Marinazzo et al., (2012), Papana et al., (2013), Papana et al., (2016), Martin et al., (2017).

(1) A coupled system of two variables with nonlinear causal effects $X_2 \rightarrow X_1$:

$$x_{1,t} = 0.3x_{1,t-1} + 0.5x_{1,t-2}x_{2,t-1} + e_{1,t}$$

$$x_{2,t} = 0.7x_{2,t-1} + e_{2,t}$$

where $e_{1,t}$, $e_{2,t}$ are independent Gaussian white noise processes with unit standard deviation (the same for all other systems). One realization of system 1 for n=1000 is displayed in Figure 2a.

(2) A coupled system of two variables with linear and nonlinear causal effects $X_2 \rightarrow X_1$, where $X_2 \sim \chi^2(8)$ and X_2 is centered to have zero mean:

$$x_{1,t} = 0.3x_{2,t-1} - 0.4x_{1,t-1} + 0.1x_{2,t-1}\, x_{1,t-1} + e_{1,t}$$

where $e_{1,t}$ is again a Gaussian white noise process with unit standard deviation (Figure 2b).

(3) A coupled system of two variables with linear asymmetric causal effect $X_{2+} \rightarrow X_1$ (Figure 2c):

$$x_{1,t} = \begin{cases} 0.3x_{1,t-1} + e_{1,t}\,, & if\ x_{2,t-1} < 0 \\ 0.2x_{1,t-1} + 0.4x_{2,t-1} + e_{1,t}, & if\ x_{2,t-1} \geq 0 \end{cases}$$

$$x_{2,t} = 0.6x_{2,t-1} + e_{2,t}$$

(4) A coupled system of two variables with non-linear asymmetric causal effects $X_{2+} \rightarrow X_1$ (Figure 2d):

$$x_{1,t} = \begin{cases} 0.4x_{1,t-1} + e_{1,t}\,, & if\ x_{2,t-1} < 0 \\ 0.3x_{1,t-1} + 0.5x_{2,t-1}^2 + e_{1,t}, & if\ x_{2,t-1} \geq 0 \end{cases}$$

$$x_{2,t} = 0.7x_{2,t-1} + e_{2,t}$$

(5) A coupled system of three variables with asymmetric causal effects $X_{2+} \rightarrow X_1$ (nonlinear) and $X_{2-} \rightarrow X_3$ (linear):

$$x_{1,t} = \begin{cases} 0.4x_{1,t-1} + e_{1,t}\,, & if\ x_{2,t-1} < 0 \\ 0.3x_{1,t-1} + 0.5x_{2,t-1}^2 + e_{1,t}, & if\ x_{2,t-1} \geq 0 \end{cases}$$

$$x_{2,t} = 0.7x_{2,t-1} + e_{2,t}$$

$$x_{3,t} = \begin{cases} 0.2x_{3,t-1} + e_{3,t}\,, & if\ x_{2,t-1} \geq 0 \\ 0.4x_{3,t-1} + 0.6x_{2,t-1} + e_{3,t}, & if\ x_{2,t-1} < 0 \end{cases}$$

The asymmetry of the couplings are generated by construction; e.g. X_2 drives X_1 only for positive values of X_2 (therefore $X_{2+} \rightarrow X_1 | X_3$), otherwise X_1 and X_2 are uncoupled (Figure 2e).

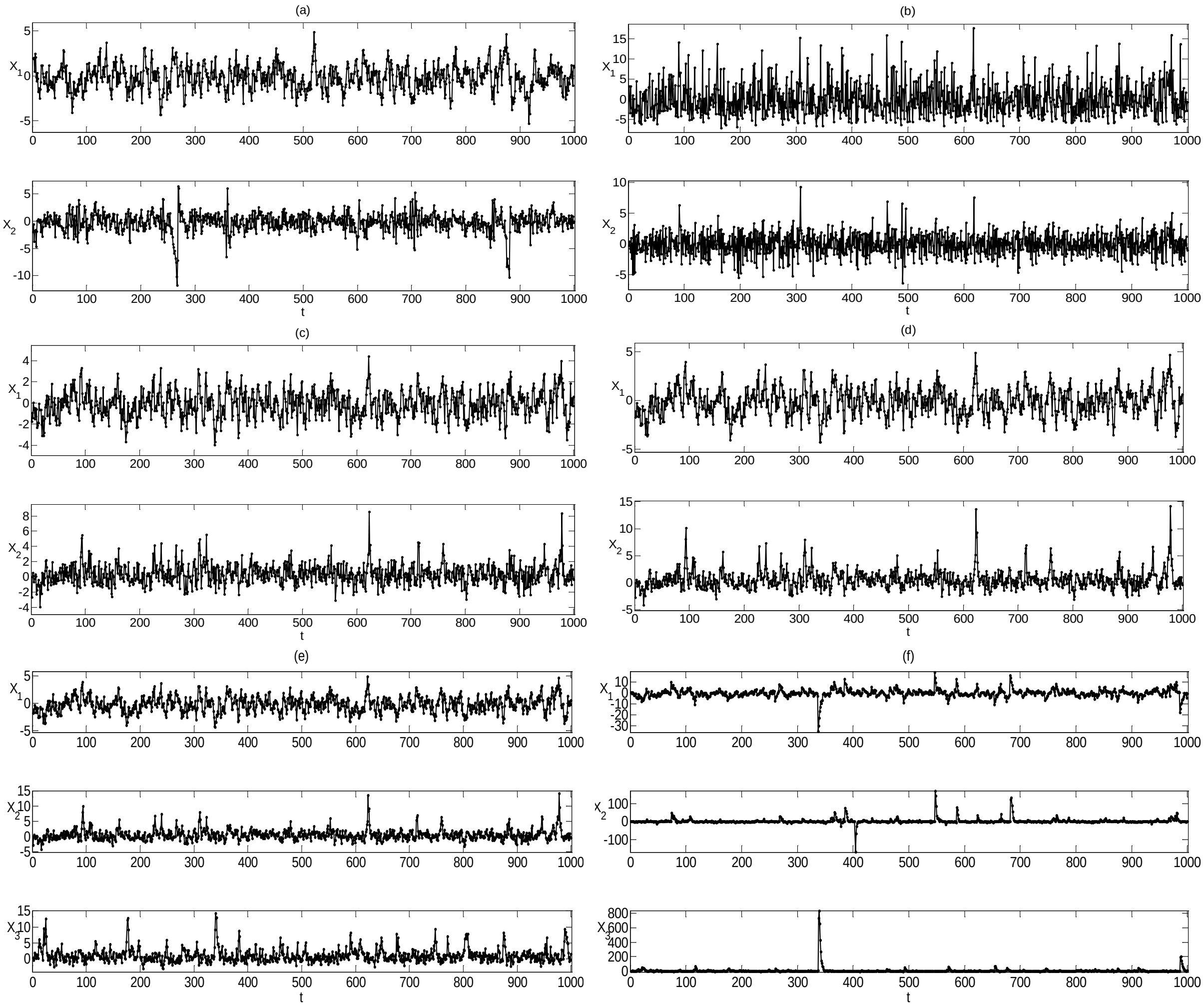

Figure 2. One realization of the simulated systems 1-6 in (a)-(f), respectively, for n=1000.

When analyzing financial time series, the presence of stylized facts can potentially affect the performance of tests. For this reason, we simulate the systems 6-8 presenting heavy tails and volatility clustering. They are defined similarly to system 5 but different noise terms are considered as follows:

(6) The noise follows a student t-distribution with 2 degrees of freedom, so that the generated series exhibits heavy tails (Figure 2f).

(7) Noise is derived from a Cauchy distribution (student t-distribution with 1 degree of freedom), so that the generated series exhibits heavier tails compared to system 6 (Figure 3a).

(8) $e_{i,t}, i = 1,2,3$, is generated by a GARCH(1,1) with

$$e_{i,t} = \sigma_t w_t$$

$$\sigma_t^2 = a_0 + a_1 e_{i,t-1}^2 + b_1 \sigma_{t-1}^2$$

where w_t is a Gaussian white noise process and $a_0 = 0.1, a_1 = 0.2, b_1 = 0.75$. Generated time series exhibits volatility clustering denoted by the α_1 coefficient (Figure 3b).

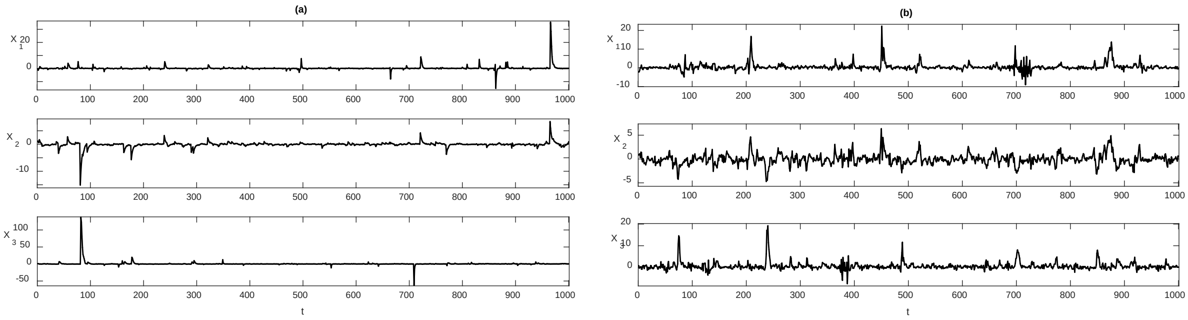

Figure 3. One realization of the simulated systems 7-8 in (a)-(b), respectively, for n=1000.

4. Results from the simulation study

In the aim to evaluate the performance of the causality tests, we display the percentage of significant values of the corresponding causality measure (rejection of the null hypothesis of non-causality) for each direction and different time series lengths *n* =1000, 2000, 4000.

System 1: The TE/ATE correctly indicate the causal effect $X_2 \rightarrow X_1$ (Table 1). Since no asymmetric couplings exists by definition, we would expect that the symmetric and the asymmetric measures perform well. TE and ATE are also estimated for embedding dimension m=2 and not only for m=1, because the equations of the system include the lagged component $x_{1,t-2}$. The TE is effective for both m and remains robust to the choice of *n* (Table 1). The percentages of significant ATE values are slightly larger for *m*=2 at the direction $X_2 \rightarrow X_1$ compared to those for m=1 and increase with *n* (see Table 2).

Table 1. Percentage of rejection of the non-causality hypothesis from 100 realizations of system 1 based on the TE.

System 1	*m*=1		*m*=2	
n	$X_1 \rightarrow X_2$	$\boldsymbol{X_2 \rightarrow X_1}$	$X_1 \rightarrow X_2$	$\boldsymbol{X_2 \rightarrow X_1}$
1000	7	**99**	9	**100**
2000	5	**100**	6	**100**
4000	8	**100**	2	**100**

Table 2. Percentage of rejection of the non-causality hypothesis from 100 realizations of system 1 based on the ATE.

	m=1			
n	$X_{1+} \to X_2$	$X_{1-} \to X_2$	$\boldsymbol{X_{2+} \to X_1}$	$\boldsymbol{X_{2-} \to X_1}$
1000	1	12	**73**	**37**
2000	7	11	**99**	**54**
4000	15	9	**100**	**74**
n	*m*=2			
1000	7	5	**87**	**58**
2000	8	3	**98**	**78**
4000	6	9	**99**	**90**

System 2: No asymmetric causality is present. Both symmetric and asymmetric causality measures detect the true couplings for all time series lengths (Tables 3 and 4). The percentage of rejection of H_0 for $ATE_{X_{2-} \to X_1}$ increases with *n*.

Table 3. Percentage of rejection of the non-causality hypothesis from 100 realizations of system 2 based on the TE (m=1).

n	$X_1 \to X_2$	$\boldsymbol{X_2 \to X_1}$
1000	4	**100**
2000	6	**100**
4000	2	**100**

Table 4. Percentage of rejection of the non-causality hypothesis from 100 realizations of system 2 based on the ATE (m=1).

n	$X_{1+} \to X_2$	$X_{1-} \to X_2$	$\boldsymbol{X_{2+} \to X_1}$	$\boldsymbol{X_{2-} \to X_1}$
1000	5	6	**98**	**83**
2000	3	7	**100**	**97**
4000	6	2	**100**	**100**

System 3: This system is defined so that only the positive values of X_2 Granger cause the corresponding X_1 observations. Although the TE finds the coupling $X_2 \to X_1$, the ATE provides further information on the predictive information of X_2 on X_1, based on the signs of the variables (Tables 5 and 6). Therefore, $ATE_{X_{2+} \to X_1}$ gives high percentages of rejection of the H_0, while low percentages are obtained with ATE for the other direction.

Table 5. Percentage of rejection of the non-causality hypothesis from 100 realizations of system 3 based on the TE (m=1).

N	$X_1 \to X_2$	$\boldsymbol{X_2 \to X_1}$
1000	3	**100**
2000	4	**100**
4000	8	**100**

Table 6. Percentage of rejection of the non-causality hypothesis from 100 realizations of system 3 based on the ATE (m=1).

n	$X_{1+} \rightarrow X_2$	$X_{1-} \rightarrow X_2$	$\boldsymbol{X_{2+} \rightarrow X_1}$	$X_{2-} \rightarrow X_1$
1000	1	6	**100**	9
2000	4	6	**100**	8
4000	7	2	**100**	11

System 4: As for the system 3, the positive values of X_2 Granger cause the corresponding X_1 observations. However, in this case causality is nonlinear. TE correctly indicates the coupling $X_2 \rightarrow X_1$ and high percentages of $ATE_{X_{2+} \rightarrow X_1}$ values are obtained (Tables 7 and 8). Again, the ATE can effectively recognize causality between two variables based on their signs.

Table 7. Percentage of rejection of the non-causality hypothesis from 100 realizations of system 4 based on the TE (m=1).

N	$X_1 \rightarrow X_2$	$\boldsymbol{X_2 \rightarrow X_1}$
1000	7	**100**
2000	7	**100**
4000	1	**100**

Table 8. Percentage of rejection of the non-causality hypothesis from 100 realizations of system 4 based on the ATE (m=1).

n	$X_{1+} \rightarrow X_2$	$X_{1-} \rightarrow X_2$	$\boldsymbol{X_{2+} \rightarrow X_1}$	$X_{2-} \rightarrow X_1$
1000	11	7	**100**	3
2000	8	4	**100**	11
4000	8	6	**100**	14

System 5: It is a multivariate system in three variables. Results in Tables 9 and 10 show that both measures fully represent the true couplings with no spurious cases.

Table 9. Percentage of rejection of the non-causality hypothesis from 100 realizations of system 5 based on the PTE (m=1).

n	$X_1 \rightarrow X_2 \mid X_3$	$\boldsymbol{X_2 \rightarrow X_1 \mid X_3}$	$\boldsymbol{X_2 \rightarrow X_3 \mid X_1}$	$X_3 \rightarrow X_2 \mid X_1$	$X_1 \rightarrow X_3 \mid X_2$	$X_3 \rightarrow X_1 \mid X_2$
1000	7	**100**	**100**	3	6	6
2000	4	**100**	**100**	3	3	4
4000	3	**100**	**100**	1	6	3

Table 10. Percentage of rejection of the non-causality hypothesis from 100 realizations of system 5 based on the APTE (m=1).

n	$X_{1+} \rightarrow X_2\|X_3$	$X_{1-} \rightarrow X_2\|X_3$	$\mathbf{X_{2+} \rightarrow X_1\|X_3}$	$X_{2-} \rightarrow X_1\|X_3$
1000	7	6	**100**	7
2000	6	5	**100**	7
4000	6	7	**100**	11
n	$X_{2+} \rightarrow X_3\|X_1$	$\mathbf{X_{2-} \rightarrow X_3\|X_1}$	$X_{3+} \rightarrow X_2\|X_1$	$X_{3-} \rightarrow X_2\|X_1$
1000	11	**100**	5	6
2000	13	**100**	7	10
4000	10	**100**	8	5
n	$X_{1+} \rightarrow X_3\|X_2$	$X_{1-} \rightarrow X_3\|X_2$	$X_{3+} \rightarrow X_1\|X_2$	$X_{3-} \rightarrow X_1\|X_2$
1000	6	3	4	6
2000	0	6	6	4
4000	4	8	3	7

System 6: The sixth simulation system evaluates the performance of the examined causality tests as for system 5 but in the presence of non-Gaussian noise and specifically for data with heavy tails. The true causalities are identified correctly with both PTE and APTE (Tables 11 and 12).

Table 11. Percentage of rejection of the non-causality hypothesis from 100 realizations of system 6 based on the PTE (m=1).

n	$X_1 \rightarrow X_2\|X_3$	$\mathbf{X_2 \rightarrow X_1\|X_3}$	$\mathbf{X_2 \rightarrow X_3\|X_1}$	$X_3 \rightarrow X_2\|X_1$	$X_1 \rightarrow X_3\|X_2$	$X_3 \rightarrow X_1\|X_2$
1000	3	**100**	**100**	0	2	6
2000	4	**100**	**100**	3	12	4
4000	4	**100**	**100**	4	7	12

Table 12. Percentage of rejection of the non-causality hypothesis from 100 realizations of system 6 based on the APTE (m=1).

n	$X_{1+} \rightarrow X_2\|X_3$	$X_{1-} \rightarrow X_2\|X_3$	$\mathbf{X_{2+} \rightarrow X_1\|X_3}$	$X_{2-} \rightarrow X_1\|X_3$
1000	4	4	**100**	12
2000	3	8	**100**	10
4000	4	5	**100**	11
n	$X_{2+} \rightarrow X_3\|X_1$	$\mathbf{X_{2-} \rightarrow X_3\|X_1}$	$X_{3+} \rightarrow X_2\|X_1$	$X_{3-} \rightarrow X_2\|X_1$
1000	8	**100**	0	4
2000	14	**100**	5	5
4000	24	**100**	9	6
n	$X_{1+} \rightarrow X_3\|X_2$	$X_{1-} \rightarrow X_3\|X_2$	$X_{3+} \rightarrow X_1\|X_2$	$X_{3-} \rightarrow X_1\|X_2$
1000	0	2	1	6
2000	5	5	4	5
4000	6	5	4	4

System 7: As it can be seen in Tables 13 and 14 when for the same system as system 5 the noise distribution has heavy tails, the test still performs well and the causal effects are correctly indicated. It is notable that as the time series length increases the test performance improves as well**.**

Table 13. Percentage of rejection of the non-causality hypothesis from 100 realizations of system 7 based on the PTE (m=1).

n	$X_1 \to X_2 \mid X_3$	$\boldsymbol{X_2 \to X_1 \mid X_3}$	$\boldsymbol{X_2 \to X_3 \mid X_1}$	$X_3 \to X_2 \mid X_1$	$X_1 \to X_3 \mid X_2$	$X_3 \to X_1 \mid X_2$
1000	3	**92**	**90**	5	7	2
2000	5	**97**	**98**	4	6	3
4000	1	**98**	**100**	6	5	4

Table 14. Percentage of rejection of the non-causality hypothesis from 100 realizations of system 7 based on the APTE (m=1).

n	$X_{1+} \to X_2 \mid X_3$	$X_{1-} \to X_2 \mid X_3$	$\boldsymbol{X_{2+} \to X_1 \mid X_3}$	$X_{2-} \to X_1 \mid X_3$
1000	6	4	**95**	7
2000	4	6	**100**	6
4000	3	21	**100**	9
n	$X_{2+} \to X_3 \mid X_1$	$\boldsymbol{X_{2-} \to X_3 \mid X_1}$	$X_{3+} \to X_2 \mid X_1$	$X_{3-} \to X_2 \mid X_1$
1000	10	**99**	1	4
2000	13	**100**	0	10
4000	6	**100**	3	21
n	$X_{1+} \to X_3 \mid X_2$	$X_{1-} \to X_3 \mid X_2$	$X_{3+} \to X_1 \mid X_2$	$X_{3-} \to X_1 \mid X_2$
1000	1	6	0	4
2000	2	5	2	0
4000	0	5	0	1

System 8: Finally, when the data are derived from the same system 5 but with noise that gives rise to volatility clustering structures, both measures give 100% significant values for all n when direct causality exists (Tables 15 and 16).

Table 15. Percentage of rejection of the non-causality hypothesis from 100 realizations of system 8 based on the PTE (m=1).

n	$X_1 \to X_2 \mid X_3$	$\boldsymbol{X_2 \to X_1 \mid X_3}$	$\boldsymbol{X_2 \to X_3 \mid X_1}$	$X_3 \to X_2 \mid X_1$	$X_1 \to X_3 \mid X_2$	$X_3 \to X_1 \mid X_2$
1000	11	**100**	**100**	14	5	6
2000	19	**100**	**100**	16	11	5
4000	20	**100**	**100**	33	7	5

Table 16. Percentage of rejection of the non-causality hypothesis from 100 realizations of system 8 based on the APTE (m=1).

n	$X_{1+} \rightarrow X_2\|X_3$	$X_{1-} \rightarrow X_2\|X_3$	$\boldsymbol{X_{2+} \rightarrow X_1\|X_3}$	$X_{2-} \rightarrow X_1\|X_3$
1000	8	6	**100**	5
2000	11	5	**100**	6
4000	23	7	**100**	6
n	$X_{2+} \rightarrow X_3\|X_1$	$\boldsymbol{X_{2-} \rightarrow X_3\|X_1}$	$X_{3+} \rightarrow X_2\|X_1$	$X_{3-} \rightarrow X_2\|X_1$
1000	4	**100**	9	3
2000	1	**100**	21	9
4000	3	**100**	28	7
n	$X_{1+} \rightarrow X_3\|X_2$	$X_{1-} \rightarrow X_3\|X_2$	$X_{3+} \rightarrow X_1\|X_2$	$X_{3-} \rightarrow X_1\|X_2$
1000	9	6	3	6
2000	5	1	3	11
4000	1	5	11	4

To summarize, the PTE and its asymmetric variant APTE capture the predefined couplings in the simulated systems. Nevertheless, the APTE goes a step ahead and offers more precise information on the nature of these relationships. This result is of paramount importance when studying financial systems in which investors' interactions, information asymmetry and aggressive contagious mechanisms impact market prices and financial stability in general.

The power of the significance tests i.e. the percentage of rejection at the significance level 5% for both test statistics (TE/PTE and ATE/APTE), when there is true direct causality, is high. However, the size of both test statistics, i.e. the probability of falsely rejecting the null hypothesis, is not always at the nominal significance level (α=0.05), and specifically higher percentages than 5 were found for large n. This is a frequently reported issue with causality tests and not only for the tests using TE/PTE (e.g. see Papana et al., 2013), which shows the difficulty of the task of estimating correctly causal effects in multivariate time series.

5. Application to financial time series

We use daily data for the CBOE Volatility Index (VIX), the S&P500 index and the S&P500 volume, during the period 2/1/2004-11/3/2014. To ensure stationarity, we transform prices into logarithmic returns for VIX (X_1), and S&P500 (X_2), while the detrended time series is considered for the S&P500 volume (X_3). To detrend, we perform a linear regression of the S&P500 volume on a constant, t and t^2, where t denotes the time steps (Chen et al., 2001).

Furthermore, in the aim to filter any linear causality and focus on the nonlinear causal links, the VAR residuals of X_1, X_2, X_3 are calculated, giving Y_1, Y_2, Y_3 (see Figure 4)[3]. Because our system of real variables is trivariate, the partial versions of the TE (i.e. PTE) and the ATE (i.e. APTE) tests are jointly implemented.

The statistical significance of causality measures is extracted using 1000 surrogates, while the free parameters are set to m=1 (embedding dimension), and k=5 (number of neighbors).

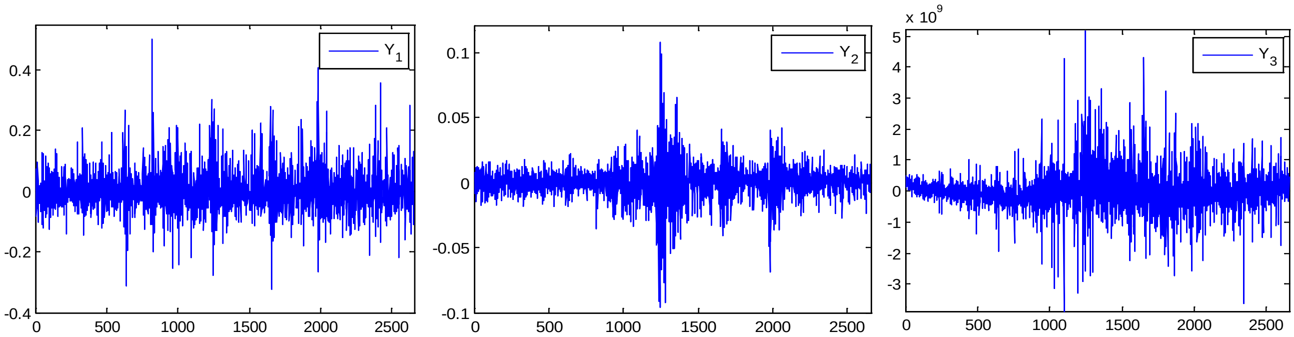

Figure 4: VAR residuals of the CBOE Volatility Index returns (Y_1), the S&P 500 returns (Y_2), and the detrended S&P500 volume (Y_3).

The p-values from the significance test for each causality measure is displayed (significance level α is set to 5%). We first examine the direct couplings among the corresponding three variables using the symmetric PTE test, revealing that $Y_1 \rightarrow Y_2|Y_3$ (i.e. VIX→S&P500) and $Y_3 \rightarrow Y_2|Y_1$ (i.e. VOL→S&P500) (Table 17). When conditioning on the signs of the driving variables, we obtain the relationship $Y_{1+} \rightarrow Y_2|Y_3$ (i.e. $VIX^+ \rightarrow$S&P500) (Table 18). Finally, we estimate the asymmetric couplings based on the APTE, conditioning on the tails of the distributions of the variables, i.e. taking into consideration only observations larger/smaller than $\mu+1\sigma$/ $\mu-1\sigma$ of the corresponding driving variable, respectively[4]. In this case, we identify the direct causal links $Y_{1-} \rightarrow Y_2|Y_3$ (i.e. $VIX^- \rightarrow$S&P500), $Y_{2+} \rightarrow Y_1|Y_3$ ($S\&P500^+ \rightarrow$VIX), $Y_{2-} \rightarrow Y_1|Y_3$ ($S\&P500^- \rightarrow$VIX) and $Y_{3+} \rightarrow Y_2|Y_1$ (i.e. $VOL^+ \rightarrow$S&P500) (Table 19).

[3] The impact of VAR filtering and bleaching of data in general is an important issue. Specially, when time series present mixed structures and since the superposition principle does not hold no filtering can leave clean residuals. However, in financial applications removing linear structures has crucial theoretical value since behavioural interpretation of the interdependences makes sense when nonlinearity prevails. In addition, the estimation of information-theoretical quantities, such as transfer entropy, is typically improved by diminishing long-range second-order temporal structure using VAR filters (Papana et al., 2016; Gomez-Herrero, 2010).

[4] The length together with the extent of asymmetry of financial time series used in our application determine the upper limit of the selected threshold.

Table 17. P-values from the significance test based on the PTE.

$\boldsymbol{Y_1 \to Y_2 \mid Y_3}$	$Y_2 \to Y_1 \mid Y_3$	$Y_2 \to Y_3 \mid Y_1$	$\boldsymbol{Y_3 \to Y_2 \mid Y_1}$	$Y_1 \to Y_3 \mid Y_2$	$Y_3 \to Y_1 \mid Y_2$
0.0077*	0.7766	0.0995	**0.0027***	0.3692	0.8995

Table 18. P-values from the significance test based on the APTE conditioning on positive/negative signs of the variables.

$\boldsymbol{Y_{1+} \to Y_2 \mid Y_3}$	$Y_{1-} \to Y_2 \mid Y_3$	$Y_{2+} \to Y_1 \mid Y_3$	$Y_{2-} \to Y_1 \mid Y_3$
0.0276	0.7327	0.8935	0.7137
$Y_{2+} \to Y_3 \mid Y_1$	$Y_{2-} \to Y_3 \mid Y_1$	$Y_{3+} \to Y_2 \mid Y_1$	$Y_{3-} \to Y_2 \mid Y_1$
0.2184	0.1784	0.2593	0.3133
$Y_{1+} \to Y_3 \mid Y_2$	$Y_{1-} \to Y_3 \mid Y_2$	$Y_{3+} \to Y_1 \mid Y_2$	$Y_{3-} \to Y_1 \mid Y_2$
0.8435	0.0686	0.8196	0.6408

Table 19. P-values from the significance test based on the APTE conditioning on the tails.

$Y_{1+} \to Y_2 \mid Y_3$	$\boldsymbol{Y_{1-} \to Y_2 \mid Y_3}$	$\boldsymbol{Y_{2+} \to Y_1 \mid Y_3}$	$\boldsymbol{Y_{2-} \to Y_1 \mid Y_3}$
0.2928	**0.0165**	**0.0461**	**0.0067**
$Y_{2+} \to Y_3 \mid Y_1$	$Y_{2-} \to Y_3 \mid Y_1$	$\boldsymbol{Y_{3+} \to Y_2 \mid Y_1}$	$Y_{3-} \to Y_2 \mid Y_1$
0.9539	0.9440	**0.0067**	0.9637
$Y_{1+} \to Y_3 \mid Y_2$	$Y_{1-} \to Y_3 \mid Y_2$	$Y_{3+} \to Y_1 \mid Y_2$	$Y_{3-} \to Y_1 \mid Y_2$
0.7861	0.7072	0.0659	0.9341

The dominance of the positive values of volume along with the negative values of S&P500 (with the $\mu \pm 1\sigma$ threshold), and the positive values of VIX (without the $\mu \pm 1\sigma$ threshold) coincides with their univariate distributional characteristics and more specifically with their skewness values, as reported in Table 20. When conditioning on the tails, decreasing VIX returns nonlinearly cause the S&P500. This result puts forward Verado (2009) findings supporting that high prior uncertainty accumulated by investors feed stock returns reversals, but informative priors (i.e. low uncertainty) can lead to returns continuation (momentum), as well.

Table 20. Descriptive statistics of the financial variables

Descriptive Statistics	**VIX returns**	**S&P500 returns**	**Detrended Volume**
Skewness	0.69049	-0.333222	1.151439
Kurtosis	7.541215	14.62311	7.424162
Jarque-Bera	2494.233	15005.50	2754.031
Probability	0.000000	0.000000	0.000000

6. Conclusion

The new asymmetric partial transfer entropy test conditions on the causing series being non-negative or non-positive. In the effort to shed more light on the impact of tail behaviour, the conditioning is extended by considering only observations exceeding a predefined threshold ($\mu\pm1\sigma$). Its performance is evaluated through simulation experiments. Coupled systems with symmetric and asymmetric causality are used containing both linear and nonlinear couplings. As expected, the superiority of the APTE is validated in the case of asymmetric systems.

The estimation of the APTE on the trivariate system, comprising the daily S&P500, VIX and volume time series, reveals very interesting couplings, mainly when extreme observations are taken into account. More specifically, nonlinear direct causal relationships are detected from the negative S&P500 returns to the VIX returns addressing the leverage hypothesis. The latter hypothesis is confirmed in US high-frequency data by Dufour et al., (2012), who use both realised and implied volatility. On the other hand, similar in direction evidence but less statistically significant, is found in the case of positive S&P500 returns. Both relationships mirror the behavioural explanation of the financial euphoria and stock market collapse relying upon the contribution of momentum strategies to the upper and lower phases of a bubble (Kyrtsou and Mikropoulou, 2014). In addition, it appears that increasing volume impacts directly S&P500, attributing a more behavioural dimension to the stock return-volume relationship (Hibbert et al., 2008). After conditioning on the tails and visualizing the dominant path diagram between volume, VIX and S&P500, it arises that the driving variable (the "risk factor") of the system is the rising volume (Figure 5).

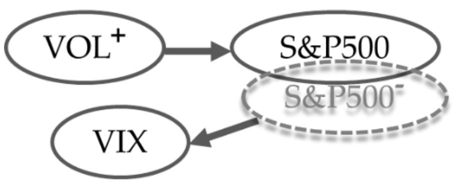

Figure 5: Path diagram of the trivariate financial system.

The detected causal channel highlights the contribution of noise trading to large swings in financial markets, via the increase of trading volume and the subsequent worsening ability of market prices to adjust to new information (Bloomfield and O'Hara, 2009; Yeh and Yang, 2011).

References

Arnhold, J., Grassberger, P., Lehnertz, K. and Elger, C., (1999): A Robust Method for Detecting Interdependences: Application to Intracranially Recorded EEG, *Physica D*, 134, pp. 419–430.

Baccala, L., and Sameshima, K., (2001): Partial Directed Coherence: A new Concept in Neural Structure Determination, *Biological Cybernetics*, 84, pp.463–474.

Black, F., (1976): Studies of stock market volatility changes, *Proceedings of the American Statistical Association, Business and Economic Statistics Section*, pp. 177–181.

Blinowska, K., Kus, R., and Kaminski, M., (2004): Granger Causality and Information Flow in Multivariate Processes, *Physical Review*,70, 050902.

Bloomfield, R., and O'Hara, M., (2009): How Noise Trading Affects Markets: An Experimental Analysis, *Review of Financial Studies*, vol. 22(6), pp. 2275-2302.

Campbell, J.Y., Hentschel, L., (1992): No news is good news: An asymmetric model of changing volatility in stock returns, *Journal of Financial Economics*, 31, pp. 281–318.

Chen G.-M., Firth, M., and Rui, M., (2001): The dynamic relation between stock returns, trading volume, and volatility, *The Financial Review*, 38, pp. 153-174.

Chiang, S-M., (2012): The relationships between implied volatility indexes and spot indexes, *Procedia-Social and Behavioral Sciences*, vol. 57, pp. 231-235.

Chuang, C-C., Kuan, C-M., and Lin, H-Y., (2009): Causality in quantiles and dynamic stock return–volume relations, *Journal of Banking and Finance*, 33 pp. 1351–1360.

De Long, J., Shleifer, A., Summers, L., Waldmann, R., (1990): Noise trader risk in financial markets, *Journal of Political Economy*, 98, pp.703–738.

Diks, C., and Panchenko, V., (2006): A new statistic and practical guidelines for nonparametric Granger causality testing, *Journal of Economic Dynamics and Control*, 30, pp.1647–1669.

Duffee, G., (1992): Trading volume and return reversals, *Working paper*, Federal Reserve Board.

Dufour, J.M., Garcia, R., Taamouti, A., 2012. .Measuring Causality between Volatility and Returns with High Frequency Data., *Journal of Financial Econometrics*, Vol. 10, No. 1, 124-163.

Eichler, M., (2013): Causal inference with multiple time series: Principles and problems, *Philosophical Transactions of the Royal Society A: Mathematical, Physical and Engineering Sciences*, 371 (1997), art. no. 20110613.

Faes, L., Porta, A., Nollo, G. (2008): Mutual nonlinear prediction as a tool to evaluate coupling strength and directionality in bivariate time series: Comparison among different strategies based on k nearest neighbors, *Physical Review E*, 78(2), art. no. 026201.

Faes, L., Nollo, G., and Porta, A., (2011): Information-based detection of nonlinear Granger causality in multivariate processes via a nonuniform embedding technique. *Physical Review E*, *83*(5), 051112.

Gomez-Herrero, G. (2010). Brain connectivity analysis with EEG. Ph.D. Thesis, Tampere University of Technology, Finland.

Granger, C., (1969): Investigating causal relations by econometric models and cross-spectral methods, *Econometrica*, 37, pp. 424-438.

Guo S., Seth A., Kendrick, K., Zhou C., and Feng, J., (2008): Partial Granger Causality - Eliminating Exogenous Inputs and Latent Variables, *Journal of Neuroscience Methods*, 172, pp. 79–93.

Hatemi-J., A., (2012): Asymmetric causality tests with an application, *Empirical Economics*, 43, pp. 447–456.

He, L-Y., Yang, S., Xie, W-S., and Han Z-H., (2014): Contemporaneous and asymmetric properties in the price-volume relationships in China's agricultural futures markets, *Emerging Markets Finance and Trade*, vol. 50, pp. 148-166.

He, L-Y., and Wen, X-C., (2015): Predictability and market efficiency in agricultural futures markets-a perspective from price-volume correlation based on wavelet coherency analysis, *Fractals*, 23 (2), 1550003: 1-14.

Hibbert, A-M., Daigler, R., and Dupoyet, B., (2008): A behavioral explanation for the negative asymmetric return–volatility relation, *Journal of Banking and Finance*, 32, pp. 2254–2266.

Hristu-Varsakelis, D., and Kyrtsou, C., (2008): Evidence for nonlinear asymmetric causality in US inflation, metal, and stock returns, *Discrete Dynamics in Nature and Society*, doi: 10.1155/2008/138547.

Hsiao, C., (1982): Autoregressive Modeling and Causal Ordering of Economic Variables, *Journal of Economic Dynamics and Control*, 4, pp. 243-259.

Kyrtsou, C., and Mikropoulou, C., (2014): Diversity, Uncertainty and Stock Market Dynamics, *Conference on Macro and Financial Economics/Econometrics*, London, May 28-30.

Kyrtsou, C., Mikropoulou, C., and Papana, A., (2016): Does the SP500 index mirror the crude oil dynamics? A complexity-based approach, *Energy Economics*, 56, pp. 239–246.

Marinazzo, D., Pellicoro, M., and Stramaglia, S., (2012): Causal information approach to partial conditioning in multivariate data sets, *Computational and mathematical methods in medicine*, Article ID 303601.

Martin, E.A., Hlinka, J., Meinke, A., Děchtěrenko, F., Tintěra, J., Oliver, I., and Davidsen, J., (2017): Network inference and maximum entropy estimation on information diagrams, *Scientific reports*, *7*(1), 7062.

Merrill, R.M., and Timmreck, T.C., (2006): *Introduction to Epidemiology*, Jones & Bartlett Learning.

Papana, A., Kugiumtzis, D., and Larsson, P.G., (2012): Detection of direct causal effects and application in the analysis of electroencephalograms from patients with epilepsy, *International Journal of Bifurcation and Chaos*, 22(9), 1250222.

Papana, A., Kyrtsou, C., Kugiumtzis, D., and Diks, C., (2013): Simulation study of direct causality measures in multivariate time series, *Entropy*, 15(7), pp. 2635-2661.

Papana, A., Kyrtsou, C., Kugiumtzis, D., and Diks, C., (2016): Detecting causality in non-stationary time series using partial symbolic transfer entropy: Evidence in financial data, *Computational Economics*, vol. 47(3), pp 341-365.

Papana, A., Kyrtsou, C., Kugiumtzis, D., and Diks, C., (2017): Assessment of resampling methods for causality testing: A note on the US inflation behavior, *PLoS One*, 12(7), pp. e0180852.

Pearl, J., (2009): *Causality: Models, Reasoning, Inference*, New York, Cambridge University Press.

Poterba, J.M., Summers, L.H., (1986): The persistence of volatility and stock market fluctuations, *American Economic Review*, 76, pp. 1142–1151.

Quian-Quiroga, R., Arnhold, J., Grassberger, P., (2000): Learning Driver-Response Relationships from Synchronization Patterns, *Physical Review E*, 61, pp. 5142–5148.

Quian Quiroga, R., Kraskov, A., Kreuz, T., and Grassberger. P., (2002): Performance of different synchronization measures in real data: A case study on electroencephalographic signals, *Physical Review E*, 65, 041903.

Romano, M., Thiel, M., Kurths, J., von Bloh, W., (2004): Multivariate Recurrence Plots, *Physics Letters A*, 330(3–4), pp. 214–223.

Rosenblum, M., and Pikovsky, A., (2001): Detecting Direction of Coupling in Interacting Oscillators, *Physical Review E*, 64, 045202.

Schreiber, T., (2000): Measuring Information Transfer, *Physical Review Letters*, 85, pp. 461–464.

Slim, S., and Dahmene, M., (2016): Asymmetric information, volatility components and the volume-volatility relationships for the CAC40, *Global Finance Journal*, vol. 29, pp. 70-84.

Vakorin, V., Krakovska, O., and McIntosh, A., (2009): Confounding Effects of Indirect Connections on Causality Estimation, *Journal of Neuroscience Methods*, 184, pp. 152-160.

Verado, M., (2009): Heterogeneous Beliefs and Momentum Profits, *Journal of Financial and Quantitative Analysis*, 44(4), pp. 795–822.

Vicente, R., Wibral, M., Lindner, M., and Pipa, G. (2011). Transfer entropy—a model-free measure of effective connectivity for the neurosciences, *Journal of Computational Neuroscience*, *30*(1), pp. 45-67.

Vlachos, I., and Kugiumtzis, D., (2010): Non-Uniform State Space Reconstruction and Coupling Detection, *Physical Review E*, 82, 016207.

Whaley, R., (2000): The investor fear gauge, *Journal of Portfolio Management*, 26, pp. 12–17.

Yeh, C.-H., and Yang, C.-Y., (2011): Examining the effects of traders' overconfidence on market behaviour, in S.-H. Chen et al. (eds.), *Agent-Based Approaches in Economic and Social Complex Systems VI: Post-Proceedings of The AESCS International Workshop 2009,* Agent-Based Social Systems 8, DOI 10.1007/978-4-431-53907-0 2, pp. 19-31.

Yu, G.-H., and Huang, C.-C., (2001): A distribution free plotting position, *Stochastic Environmental Research and Risk Assessment*, 15, pp. 462–476.